Hydrological Science and Technology, Volume 22, No. 1-4
Journal of the American Institute of Hydrology

MULTI-DIRECTIONAL ANALOGS OF TWO-DIMENSIONAL FLOW

T. V. HROMADKA, II
Department of Mathematical Sciences, United States Military Academy, West Point, NY
Professor Emeritus, California State University, CA, USA
Phone: 714-241-0099 Fax: 714-241-0092
Email: ted@phdphdphd.com

R. J. WHITLEY
Department of Mathematics, University of California, Irvine, CA, USA
Phone: 206-780-3092
Email: rwhitley@math.uci.edu

N. JORDAN
Exponent Failure Analysis
Irvine, CA, USA
Phone: 949-341-6012 Fax: 949-341-6059
Email: njordan@exponent.com

ABSTRACT

With increasing use of automated information systems such as Geographic Information Systems coupled with hydrologic and hydraulics modeling packages, floodplain analysis is becoming more dependent upon the application of computer hydraulic floodplain analysis tools.

These hydraulic analysis tools are numeric solutions of the one-dimensional and two-dimensional flow equations. Of particular interest in this paper are the mathematical underpinnings of the two-dimensional type of hydraulics models based upon use of multi-directional flow analogs. Such models typically discretize the topography of the study area into hundreds or thousands of geometrically regular polygons that "tile" the study area (that is, leaving no "gaps"). Then, the governing flow equations are numerically solved on each tile. When applied to a simple steady-state problem of uniform flow in a hydraulically wide (i.e., where hydraulic edge effects are negligible) flow regime of constant topographic slope and constant friction factor, where Manning's equation is assumed to apply, it is shown that the "4-direction" flow analog built of tiled squares matches the results of Manning's equation exactly, whereas other multi-directional flow analogs may produce biased hydraulic results.

INTRODUCTION

Many hydraulic computer models are available for use in floodplain analysis. Most of these models can be classified as being either one-dimensional (1D) or two-dimensional (2D) flow models, and can be further classified as steady or unsteady flow models, among other categorizations. Of the two-dimensional unsteady flow models, either finite element or finite difference numerical techniques are typically employed to solve the governing flow equations. These flow analogs are then applied to an array of cells or tiles of regular polygon shape that completely tile the problem domain (i.e., leaving no "gaps") in order to model the topographic flow component of the floodplain. Some models include a 1D channel routing sub-model that interfaces with the topographic or overland flow 2D model (e.g., Hromadka and Yen, 1987), but only the 2D model component is considered in this paper. Because a GIS program can readily discretize a wide scale topographic database into a dense edge-to-edge or "stacked" grid or cell coverage (similar to a tile coverage of a floor), use of such 2D analogs is oftentimes attractive.

The earliest example known to the authors of such a coupled 1D channel and 2D topographic unsteady flow model is the Diffusion Hydrodynamic Model (or DHM) published in 1987 as a USGS Water Resources Investigation (Hromadka and Yen, 1987). The DHM includes a coupled 1D channel routing and 2D topographic flow model that uses a "4-direction" flow analog based upon square grid elements or cells. Other discussions of the DHM can be found in the Handbook of Hydraulics (Brater et al, 1996, Chapter 14) and the Handbook of Hydrology (D.R. Maidment, 1993, Chapter 21).

As shown in example problems in the cited USGS DHM report, it is possible to refine the surface modeling by rotating each cell slightly to align with the contour lines and flow streamlines of the problem under study. This refinement is productive in small models, where a GIS program is not used to discretize a topographic database. The refinement where DHM grids are aligned such that the principal analog flow directions align with the topographic gradients is not considered in this paper.

A "4-direction" cell coverage of square cells, such as that used the DHM model, is the baseline model considered in this paper. The typical DHM cell and connections to neighboring cells is shown in Figure 1, illustrating a grid coverage of cells that are "stacked" in all directions along the x- and y-coordinates. This cell arrangement is typically produced by a computer discretization of a topographic database, without respect to topographic features of the floodplain. It is assumed that flow connections exist with respect to each cell's orientation in the north, east, south, and west (N, E, S, W) directions where the central cell is labeled "c" in Figure 1. Because the DHM is solving the governing flow equations by an integrated finite difference method application of flow along streamlines, it is assumed that the DHM cells are oriented such that either the N-S or E-W flow directions of a grid align with the streamlines of the flowfield anticipated. Figure 6a illustrates the assumed square cell in a flow field, with flow permitted to enter or exit each of the four sides of the square.

Other 2D modeling schemes include the regular triangle (see Figure 2 with Figure 6b assumed inflow) or the regular hexagon (Figures 3 and 6c) both of which have regular tiling which completely fill the problem domain. Another 2D modeling scheme might use a regular polygon, such as an octagon, filled inside a square tile (Figures 4 and 6d), or other 2D polygons inscribed within square tiles such that the polygon has 2^m number of sides (Figures 5 and 6e). Because only regular polygon tilings are considered in this paper, only the triangle, square, hexagon, and 2^m-side regular polygons fitted into square grid tilings are analyzed.

In order to mathematically examine the various considered multi-directional flow analogs in the simplest case, these analogs are applied to the same flow field problem of a wide open channel with steady uniform flow. That is, flow does not change with respect to time and edge effects produce negligible effect in the modeled result. The topographic slope and roughness are assumed constant so that normal flow is approximated. Flow per unit width of cross section perpendicular to flow is assumed constant. See Chow, 1959, pages 26 and 27. Hereafter, the problem is noted as steady state uniform flow, or "SSUF".

It will be shown that the baseline "4-direction" flow analog matches the SSUF flow predicted by Manning's equation, whereas other multi-direction flow analogs do not match the results predicted by Manning's equation for the same SSUF. The degree of mismatch is an inherent bias or systematic error.

It is important to note that the purpose of this paper is not to introduce a new 2D discretization scheme for subsequent use, but to critically examine currently-used 2D discretization schemes. In particular, it is shown mathematically that biased results can be produced by 2D discretization schemes that are not based on a "4-direction" cell coverage of square cells.

SSUF TEST PROBLEM DETAILS

Consider steady state (or near steady state) flow in a uniform (or near uniform) flow regime, Ω, wherein streamlines are parallel and all hydraulic parameters of topographic slope, s_o, and Manning's friction factor, n, are constant. For example, the subject flow regime, Ω, may be a portion of a larger overland flow regime or be part of a much larger floodplain, R, such that the hydraulic flow boundary conditions on Ω (where Ω is interior of R), are along flow streamlines and not an edge condition such as a topographic constraint or other similar type of flow constraint. Then, although the 2D flow equations apply on R, and therefore also apply on Ω, the 2D equations can be simplified to the 1D flow equations in Ω. Therefore, because of SSUF, flow depth is constant everywhere in Ω and the flow streamlines are orthogonal to the elevation contour lines of the constant-sloped topography (with slope, s_o).

From the definition of the problem, Manning's equation applies in Ω, where all resistance to flow is assumed due to bottom friction, and neglecting the side boundary layer effects, and unit discharge, q*, per unit width of flow perpendicular to the streamline field is given by

$$q^* = \frac{1}{n} y_n^{5/3} s_0^{1/2} \qquad [1]$$

where n is the friction factor; y_n, is the "normal depth"; s_o is the topographic slope; and Equation (1) is independent of model time by the problem assumptions.

In order to mathematically examine the considered cell flow analogs, each analog will be applied to the SSUF situation, given the unit flow value, q^*, and then the resulting analog-produced flow depths will be compared to the normal depth of Equation (1).

APPLICATION OF A "4-DIRECTION" FLOW ANALOG (IN ALIGNMENT)

Figures 1 and 6a show the resulting flow components in the application of the "4-direction" flow analog to the above test problem where the flow principal directions of the flow analog align with the streamlines. Due to the SSUF assumptions, the unit flows (smaller arrows in Figure 6a) towards node C from node S equal the unit flows towards N from C, which equal the flows crossing through the interior of the cell giving the results

$$\left.\begin{aligned} q_{S\to C} &= q_{C\to N} \\ q_{W\to C} &= q_{E\to C} = 0 \end{aligned}\right\} \tag{2}$$

where the considered "4-direction" flow analog flow rates of both $q_{S\to C}$ and $q_{C\to N}$ simply reduce to application of Manning's equation (see Hromadka and Yen, 1987) and, therefore, the "4-direction" analog produced flow depth, h_4, equals the true normal depth for the test problem, y_n, giving

$$h_4 = y_n \qquad [3]$$

In Equation (3), it is again noted that the grid alignment principal flow directions coincide with the test problem streamline orientation.

APPLICATION OF A "3-DIRECTION" FLOW ANALOG (IN ALIGNMENT)

Figures 2 and 6b provide the relevant information for use of a regular triangle (equilateral) coverage of the 2D SSUF problem domain. From Figures 2 and 6b, the total actual inflow from Manning's equation, Q, can be equated to the 2D flow analog outflow by,

$$Q = Q_{C\to NW} + Q_{C\to NE} = 2Q_{C\to NE} \qquad [4]$$

For the SSUF problem under study, the analog's outflow across a side is Δq, where by the usual Manning's equation application (and where the topographic slope along arbitrary flow vector at angle α is $s_0 \sin\alpha$),

$$\Delta q = \frac{1}{n} h_3^{5/3} s_0^{1/2} \sin^{1/2}\beta\delta \qquad [5]$$

where δ is the length of the regular polygon side inscribed on the circle boundary; and β is the angle of the analog's outflow vector through the perpendicular bisector of the side. From Figure 6b, $\delta = \ell$, where ℓ is grid width (length). Also, the diagonal vector topographic slope (i.e., from node C to NE and node C to NW) is $s_o/2$. Therefore, recalling $Q = \ell q^*$, Equation (5) is rewritten as

$$\frac{1}{n} y_n^{5/3} (s_o)^{1/2} \ell = 2\left(\frac{1}{n} h_3^{5/3} (s_o)^{1/2} \ell / \sqrt{2}\right) \qquad [6]$$

where h_3 is the considered "3-direction" flow analog flow depth. Reducing Equation (6) gives,

$$h_3 = \left(\frac{\sqrt{2}}{2}\right)^{3/5} y_n = 0.81 y_n \qquad [7]$$

Compare the inequality in Equation (7) with the equality in Equation (3). The three-direction flow analog produces a depth that is about 80-percent of normal depth.

APPLICATION OF A "6-DIRECTION" FLOW ANALOG (IN ALIGNMENT)

Figures 3 and 6c provide the relevant information for use of a regular hexagon tile coverage of the 2D problem domain. From Figures 3 and 6c, the total actual inflow from Manning's equation, Q, can be equated to the 2D flow analog outflow by,

$$\begin{aligned} Q &= Q_{C \to NW} + Q_{C \to N} + Q_{C \to NE} \\ &= Q_{C \to N} + 2\, Q_{C \to NE} \end{aligned} \qquad [8]$$

From the Figures 3 and 6c, $\delta = 1/2$. Then Equation (8) is rewritten as

$$\frac{1}{n} y_n^{5/3} (s_0)^{1/2} \ell = \left[\frac{1}{n} h_6^{5/3} (s_0)^{1/2} \ell / 2\right] + 2\left[\frac{1}{n} h_6^{5/3} (s_0)^{1/2} \ell / \sqrt{2}\right] \qquad [9]$$

where h_6 is the considered "6-direction" flow analog flow depth. Reducing Equation (9) gives,

$$h_6 = \left(\frac{2\sqrt{2}}{2+\sqrt{2}}\right)^{3/5} y_n \approx 0.89\, y_n \qquad [10]$$

Compare the inequality in Equation (10) with the equality in Equation (3). The 6-direction flow analog produces a depth that is about 90-percent of normal depth.

APPLICATION OF AN "8-DIRECTION" FLOW ANALOG (IN ALIGNMENT)

Of the multi-directional flow analogs considered, the regular triangle, square, and hexagon cells can be used to completely tile a problem domain. The octagon and other regular 2^m-side cells cannot, without further enhancement to insure that the entire surface of the problem domain is tiled without gaps or overlaps that would lead to continuity errors. For example, the octagon cell, m=3, can be fitted inside a square tile. Because the "8-direction" flow analog is the next simplest scheme, it is analyzed next. The resulting mathematical simplifications obtained from the "8-direction" flow analog analysis are then extended to the arbitrary 2-regular sided polygon, and as m approaches infinity (i.e., a circle cell).

Figures 4 and 6d show the model flow components in the application of the considered "8-direction" flow analog, in the alignment, to the above test problem. The flows crossing through the interior of the octagon cell are set equal to the sum of the three unit flow components in the directions of node C to NE, C to N, and C to NW given by $q_{C \to NE}$, $q_{C \to N}$, $q_{C \to NW}$ respectively. That is, flows are computed "due N" and also on two diagonals. By symmetry, the diagonal unit flows of the analog match, giving

$$q_{C \to NE} = q_{C \to NW} \qquad [11]$$

Under the problem assumptions, there should be zero flow to the NE and NW grids from the C grid. However, the considered "8-direction" flow analog computes flow rates based on gradients between the cell network nodes and therefore the analog's diagonal flows, are not necessarily zero.

The flow length of the analog flow direction boundaries, δ, are computed by noting for grid width (and length), ℓ, octagon side length δ is found by (see Figure 6d)

$$2\frac{\delta}{\sqrt{2}}+\delta=\ell \qquad [12]$$

or

$$\delta=\frac{\ell}{1+\sqrt{2}} \qquad [13]$$

the topographic slope from C to N is s_o, therefore, the topographic slope from C to NE (or C to NW) is $s_o/\sqrt{2}$. Because flow depths are constant throughout Ω (SSUF), application of Manning's equation along the flow path prescribed by each flow direction of the flow analog gives the unit flows crossing the octagon boundary (including the considered analog's diagonal flowpath) gives,

$$q_{C\rightarrow NW}=q_{C\rightarrow NE}=\frac{1}{n}h_8^{5/3}\left(s_0/\sqrt{2}\right)^{1/2} \qquad [14]$$

and

$$q_{C\rightarrow N}=\frac{1}{n}h_8^{5/3}\left(s_0\right)^{1/2} \qquad [15]$$

where h_8 is the "8-direction" flow depth that is also uniform in Ω.

The total outflow of the octagon is given from Equations (14) and (15),

$$Q_{C\rightarrow NW}=Q_{C\rightarrow NE}=\delta q_{C\rightarrow NE} \qquad [16]$$

$$Q_{C\rightarrow N}=\delta q_{C\rightarrow N} \qquad [17]$$

where $Q_{C\rightarrow N}$, for example, is the analog's total flow rate from C to N. Similarly, the actual total flow, Q, through the octagon cell is given from Equation (1) and Figure 6d by

$$Q=\ell q^{*} \qquad [18]$$

Equating octagon cell outflow to the flow through the cell, Q, from Equations (1) and (14) through (18), gives

$$Q_{C\rightarrow NW}+Q_{C\rightarrow N}+Q_{C\rightarrow NE}=Q \qquad [19]$$

Or, after simplifying,

$$2(h_8^{5/3}/2^{1/4})\ell/(1 \quad \sqrt{2}) \quad h_8^{5/3}\ell/(1 \quad \sqrt{2}) \quad y_n^{5/3}\ell \qquad [20]$$

or, dividing by grid dimension, ℓ,

$$h_8^{5/3}\frac{2^{3/4}+1}{1+\sqrt{2}}=y_n^{5/3} \qquad [21]$$

giving the "8-direction" flow analog flow depth, h_8, as

$$h_8=\left(\frac{1+\sqrt{2}}{1+2^{3/4}}\right)^{3/5} y_n \qquad [22]$$

which gives, approximately,

$$h_8 \approx 0.939\, y_n \qquad [23]$$

That is, when the octagon cell is aligned along streamlines as shown in Figures 4 and 6d, the considered "8-direction" flow analog does not match normal depth, y_n, in Equation (1) for the SSUF test problem. The eight-direction flow analog produces a depth that is about 94-percent of normal depth.

ALTERNATIVE 8-DIRECTION FLOW ANALYSIS

The prior analysis of the SSUF problem can be recast into simply the simultaneous application of Manning's equation on each of the considered "8-direction" flow analog's principal flow directions. Using the terms and components of the previous analysis,

$$\frac{Q_{C\to N}}{Q_{C\to NW}}=\left(\frac{s_0}{s_0/\sqrt{2}}\right)^{1/2}=2^{1/4} \qquad [24]$$

where the length of the diagonal flow path between local nodes C and NW is $\ell\sqrt{2}$. Therefore, the outflow from local cell, C, for the SSUF test problem, is

$$Q_{C\to NW}+Q_{C\to N}+Q_{C\to NE}=Q_{C\to N}\,(1+2^{3/4}) \qquad [25]$$

The considered "8-direction" flow analog flow rate $Q_{C\to N}$ is, from Equation (13), (15), (17), given by

$$Q_{C\to N}=\frac{1}{n}s_0^{1/2}\ell h_8^{5/3}/\left(1+\sqrt{2}\right) \qquad [26]$$

Combining Equations (25) and (26) gives the total analog outflow from the octagon cell in grid cell C as

$$\text{Outflow}=\frac{1}{n}s_0^{1/2}\,\ell\, h_8^{5/3}\,(1+2^{3/4})/(1+\sqrt{2}) \qquad [27]$$

From Equations (1) and (18), total flow, Q, through cell C is

$$Q=\frac{1}{n}s_0^{1/2}\,\ell\, y_n^{5/3} \qquad [28]$$

From Equations (27) and (28) and simplifying,

$$h_8 = \left(\frac{(1+\sqrt{2})}{(1+2^{3/4})} \right)^{3/5} y_n \qquad [29]$$

which matches the results derived in Equation (22). This second derivation will be used for the other cell and tile analyses.

APPLICATION OF A 2^M-SIDED REGULAR POLYGON FLOW ANALOG

The formulation for the "8-direction" flow analog can be extended to a 2^m-sided regular polygon by fitting a circle inside the square tile and using the geometric properties of the polygon fitted to the circle. For m=3, an octagon results. However in the previous analysis, the octagon can also be inflated outside of the circle cell and fitted to the square grid tile directly. For either case, the resulting formulations are analogous.

For the 2^m-sided regular polygon (m an integer greater than 2) oriented such that there are sides parallel with both the x- and y-axis, the radius of the circle is $\ell/2$, where ℓ is the grid tile dimension.

For the SSUF problem under study, the analog's outflow across a side is Δq, where by the usual Manning's equation application,

$$\Delta q = \frac{1}{n} h_{2^m}^{5/3} s_0^{1/2} \sin^{1/2}\beta\delta \qquad [30]$$

where δ is the length of the regular polygon side inscribed on the circle boundary; and β is the angle of the analog's outflow vector through the perpendicular bisector of the side. From the polygon orientation,

$$\delta = 2\left(\frac{\ell}{2}\right)\sin\left(\frac{2\pi}{2^m}\frac{1}{2}\right) \qquad [31]$$

Simplify by letting K be defined by

$$K = \frac{1}{n} h_{2^m}^{5/3} s_0^{1/2} \ell \sin\left(\frac{\pi}{2^m}\right) \qquad [32]$$

then the total outflow from the polygon, using symmetry, is

$$\text{outflow} = 2\sum_{i=1}^{(2^{m-2}-1)} (K\sin^{1/2}\beta_i) + K \qquad [33]$$

where β_i is the angle (with respect to the x-axis) to the vector that is the perpendicular bisector of polygon side i. Note that there are $(2^{m-2}-1)$ polygon sides that are totally contained in the first quadrant, with one side on the top and parallel with the x-axis such that its perpendicular bisector aligns with the y-axis (and hence the singleton term K, in Equation (33)). That is, the polygon is in "alignment" with the flow streamlines.

For β_1, $\beta_1 = \pi/2^{m-1}$ (e.g., for the octagon cell, there is only β_1 to deal with, m=3, and $\beta_1=\pi/4$). Similarly, for m $\geq$3,

$$\beta_i = i\pi / 2^{m-1}; i = 1, 2, \ldots, \left(2^{m-2} - 1\right) \qquad [34]$$

Then, Equations (33) and (34) can be combined as

$$\text{outflow} = K\left[(2\sum_{i=1}^{(2^{m-2}-1)} \sin^{1/2}(i\pi / 2^{m-1})) + 1 \right] \qquad [35]$$

Because of the polygon alignment within the grid (as inscribed in the circle), the projected width of inflow, ℓ^*, with respect to the streamlines is shortened to be less than grid dimension, l, by

$$\ell^* = \ell\cos(\pi/2^m) \qquad [36]$$

Then, inflow to the polygon is

$$\text{inflow} = \frac{1}{n}\, y_n^{5/3} s_o^{1/2} \ell \cos(\pi / 2^m) \qquad [37]$$

Equating inflow to the "2^m-direction" analog outflow for the considered SSUF problem gives

$$\frac{1}{n} y_n^{5/3} s_o^{1/2} \ell \cos(\pi / 2^m) = \left[\frac{1}{n} h_{2^m}^{5/3} s_o^{1/2} \ell \sin(\pi / 2^m)\right] * \left[(2\sum_{i=1}^{2^{m-2}-1} \sin^{1/2}(i\pi/2^{m-1})) + 1 \right] \qquad [38]$$

or simplifying,

$$y_n^{5/3}\cos\left(\pi/2^m\right) = \left[h_{2^m}^{5/3}\sin\left(\pi/2^m\right)\right]\left[\left(2\sum_{i=1}^{2^{m-2}-1}\sin^{1/2}\left(i\pi/2^{m-1}\right)\right)+1\right]$$

giving

$$h_{2^m} = y_n / \left(\left[2\sum_{i=1}^{(2^{m-2}-1)} \sin^{1/2}(\pi / 2^{m-1}) + 1 \right] \tan(\pi / 2^m)\right)^{3/5} \qquad [39]$$

For example, for m=3 (octagon cell in alignment), Equation 39 gives

$$h_8 = y_n/([2\sin^{1/2}(\pi/4)+1]\tan(\pi/8))^{3/5} = 0.939\, y_n \qquad [40]$$

which is the result previously derived at Equation (23). (The last flow analog considered in this paper is the case $m \rightarrow \infty$). It is noted that in these geometric constructions, the projections of the control surface onto a line perpendicular to the flow direction is used to simplify flux calculations.

LETTING THE REGULAR POLYGON CELL ANALOG APPROACH A CIRCLE CELL

Of possible interest is the use of a regular m-sided polygon, fitted inside the square tile (as accomplished for m=8 previously), and let m approach infinity. Then the regular polygon approaches being a circle. The previous problem setting can be examined for the subject SSUF problem. Figures 5 and 6e depict the problem situation. From the figures, angle α corresponds to the flow analog vector outflow, $dq(\alpha)$, with corresponding flow boundary $d\delta = r d\alpha$. For the stated SSUF problem, the topographic slope along arbitrary flow vector at angle α is $s_o \sin\alpha$ (see Figure 7). Therefore,

$$dq = \frac{1}{n} h_\infty^{5/3} (s_o)^{1/2} (\sin\alpha)^{1/2} r \, d\alpha \qquad [41]$$

where dq is incremental outflow; h_∞ is the flow analog flow depth, $s_o \sin\alpha$ is the topographic slope along the vector at angle α. The inflow into the cell is Q, where

$$Q = \frac{1}{n} 2r y_n^{5/3} (s_o)^{1/2} \qquad [42]$$

The outflow from the cell is

$$\int_{\theta=0}^{\pi} dq = 2\left(\frac{1}{n} h_\infty^{5/3} (s_o)^{1/2} r\right) \int_{0}^{\pi/2} (\sin\alpha)^{1/2} d\alpha \qquad [43]$$

Setting inflow equal to outflow, the flow analog flow depth, h_∞, is

$$h_\infty = y_n \Big/ \left(\int_0^{\pi/2} (\sin\alpha)^{1/2} d\alpha \right)^{3/5} \qquad [44]$$

or approximately,

$$h_\infty \approx 0.90\, y_n \qquad [45]$$

DISCUSSION

For all but one of the considered 2D multi-direction flow analogs, it is shown that the resulting estimation of flow depth, for the considered SSUF problem, may be biased, whereas the considered "4-direction" flow analog estimation of flow depth matches the normal depth from Manning's equation. And, in this test situation, the considered flow analogs were applied such that their respective principal flow path directions are in an alignment with the streamlines of the governing flowfield. In situations where the principal flow paths are not in alignment with the streamlines of the governing flow fields there may be an associated further decrease in modeling accuracy. Therefore, in the considered flow analogs, a goal is to align the analog principal flow paths with the problem's streamlines. Unfortunately, a typical GIS "stacked" cell discretization or tiling may produce cells that are not in alignment with the governing flow field. A summary of the relevant information for the various considered flow analogs is provided in Table 1.

For the case of shallow overland flow, it has been shown (Engman, 1989) that the governing flow equations can be solved with proper boundary conditions and the selection of only one parameter, Manning's n. Accordingly, friction factor may be adjusted so that computed depths match actual depths. In general, all 2m-sided polygons except the square (m=2) calculate SSUF flow depths that are 80-percent to 94-percent of the theoretical normal depth. The resulting bias in hydraulic results might be smaller than other uncertainties in the hydraulic modeling process, and might pass unnoticed. Bias is eliminated or reduced by calibration of the mathematical model to actual flow depths, usually by adjusting the friction factor. Theoretically, and as a first approximation, the friction factor would be reduced in proportion to the correction based on polygon side "j" to produce a corresponding increase in flow depth. The adjustments in friction factor in some cases would be less than the published variation in friction factor.

CONCLUSIONS

The convenience of using GIS tools to develop dense discretizations or tilings of topographic layouts, resulting in hundreds and thousands of uniformly "stacked" modeling grid cells or tiles that cover the topographic layout of a floodplain problem, has resulted in increasing use of two-dimensional flow hydraulics models such as DHM and other models. However, the underpinnings of the flow analogs used in such two-dimensional flow models require satisfying the governing flow equations, including satisfying flow constraints with respect to flow streamlines.

The mathematical analysis of several considered multi-directional flow analogs as applied to a simple test problem indicate that when cells or tiles are aligned with flow streamlines, such as shown in the test applications, the considered "4-direction" analog results match those from Manning's equation whereas the results from other considered multi-directional flow analogs underestimate normal depths calculated from Manning's equation. Because alignment of computational cell principal flow directions with flow streamlines would enable better approximations, there may be a degradation in accuracy in the considered modeling analogs results if cells are not aligned with the streamlines of the flow regime. There is a tradeoff, however, because the accuracy increase from aligning each cell with flow streamlines must be weighed against the accuracy increase from many more small cells aligned without respect to flow streamlines. Adjustment of the friction factor so that computed flow depths match actual flow depths provides a way to reduce bias where computer-generated gridding (i.e., automated "tiling" of a watershed flow path regime) does not align with flow streamlines.

Nonetheless, for the test problem examined, the considered "4-direction" flow analog results did match results from Manning's equation whereas the other considered multi-directional flow analogs did not. It would be anticipated that adjustments of friction factor for "4-direction" flow would be less than for other multi-directional flow analogues.

It is noted that in this paper, not all possible tiling and flow analog schemes are examined.

REFERENCES

Brater, E.F., King, H.W., Lindell, J.E., Wei, C.Y., 1996, Handbook of Hydraulics, McGraw-Hilll, Seventh Edition, Chapter 14, page 33.

Chow, V.T., 1959, Open-Channel Hydraulics. McGraw-Hill.

Engman, E. T., 1989, "The Applicability of Manning's n Values for Shallow Overland Flow", Proceedings of the International Conference on Channel Flow and Catchment Runoff: Centennial of Manning's Formula and Kuichling's Rational Formula.

Handbook of Hydrology, 1993, D.R. Maidment Editor, Chapter 21, pages 26-27.

Hromadka II, T.V. and Yen, C.C., 1987, U.S. Geological Survey Water-Resources Investigations Report 87-4137, "A Diffusion Hydrodynamic Model".

FIGURES AND TABLES

(1) j	(2) L/ℓ	(3) L_d/ℓ	(4) α	(5) s_{od}/s_o	(6) δ/ℓ	(7) k_j
3	$\sqrt{3}/3$	$\sqrt{3}/3$	$\pi/6$	1/2	1	0.81
4	1	--	--	--	1	1.00
6	$\sqrt{3}/2$	$\sqrt{3}/2$	$\pi/6$	1/2	1/2	0.89
8	1	$\sqrt{2}$	$\pi/4$	$\sqrt{2}/2$	$1/(1+\sqrt{2})$	0.94
2^m	W	various	various	$s_o$sin□□	$\Delta\delta$	Eqn.39:(8)(9)
∞	W	various	various	$s_o \sin\alpha$	$d\delta$	0.90

Notes:
(1) number or regular polygon cell sides
(2) length between nodes from C to nodes N, S, E, W
(3) diagonal length between nodes, from C, to nodes NE, NW, SE, SW
(4) diagonal flow vector angle to x-axis
(5) topographic slope along diagonal flow vector, as proportion of topography slopes, s_o
(6) regular polygon side length, as proportion of assumed inflow projected boundary, W
(7) $h_j = k_j y_n$; y_n = normal depth, k_j approximated
(8) for 2^m, let $m \geq 3$
(9) Example: for 2^m, m=4, $k_{16} = 0.91$.

Table 1. Regular Polygon Cell Flow Analog Information.

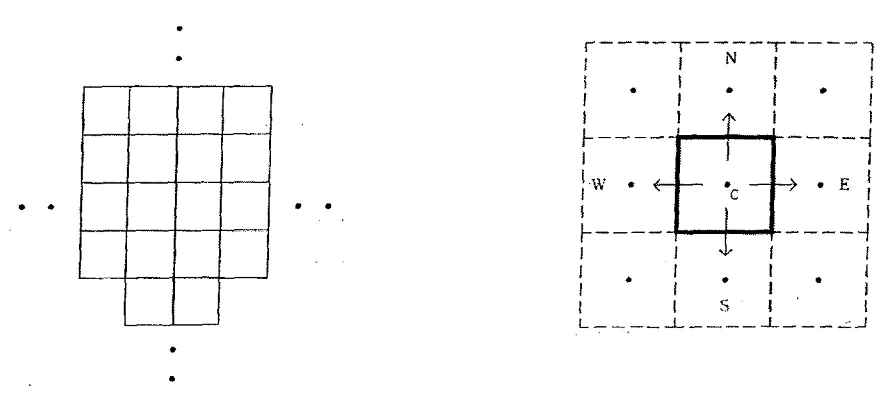

"Stacked Tiling Pattern Using Square Grid Tiles.

Figure 1. Finite - Difference Cell and Flow Directions for Square "4 – Direction" Flow Analog.

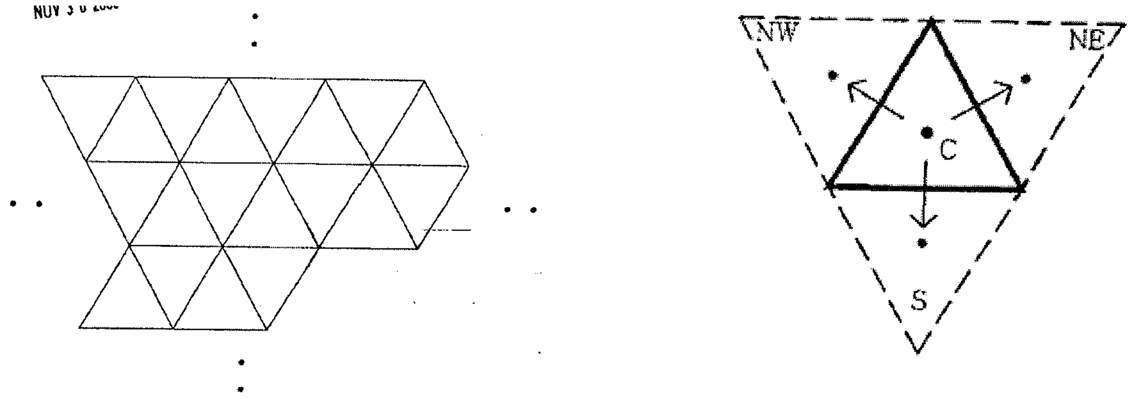

Tilting Pattern Using Regular Triangle Tiles.
Paired Dots Indicate Tiling Extending Beyond Illustration

Figure 2. Finite – Difference Cell and Flow Directions for "3 – Direction" Flow Analog.

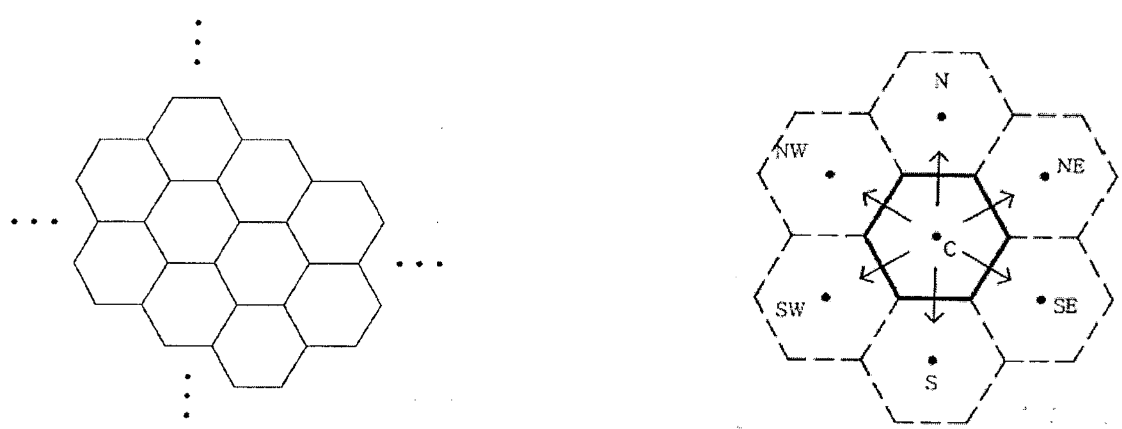

Tiling Pattern Using Regular Hexagon Tiles. Paired Dots
Indicate Tiling Extending Beyond Illustration .

Figure 3. Finite – Difference Cell and Flow Directions for "6 – Direction" Flow Analog.

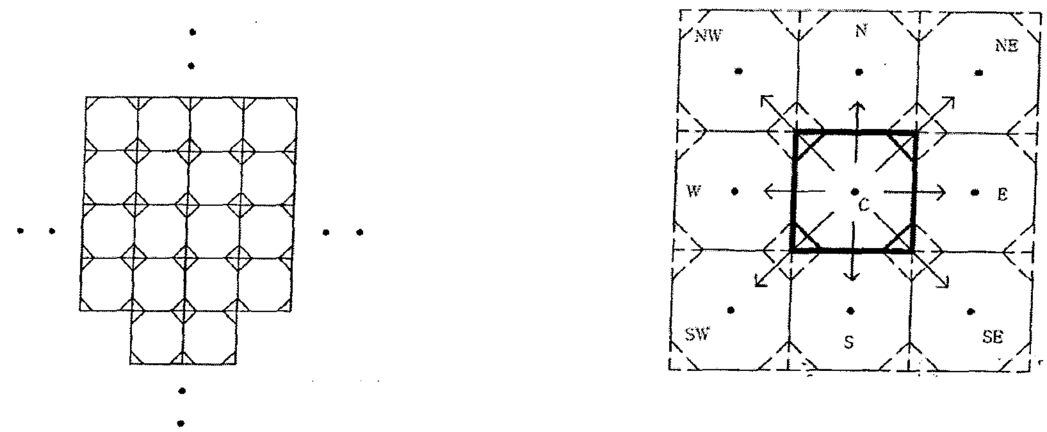

Tiling Pattern Using Regular Octagon Cell Fitted Within Square Tiles. Paired Dots Indicate Tiling Extending Beyond Illustration.

Figure 4. Finite Difference Cell and Flow Directions for "8 – Direction" Flow Analog.

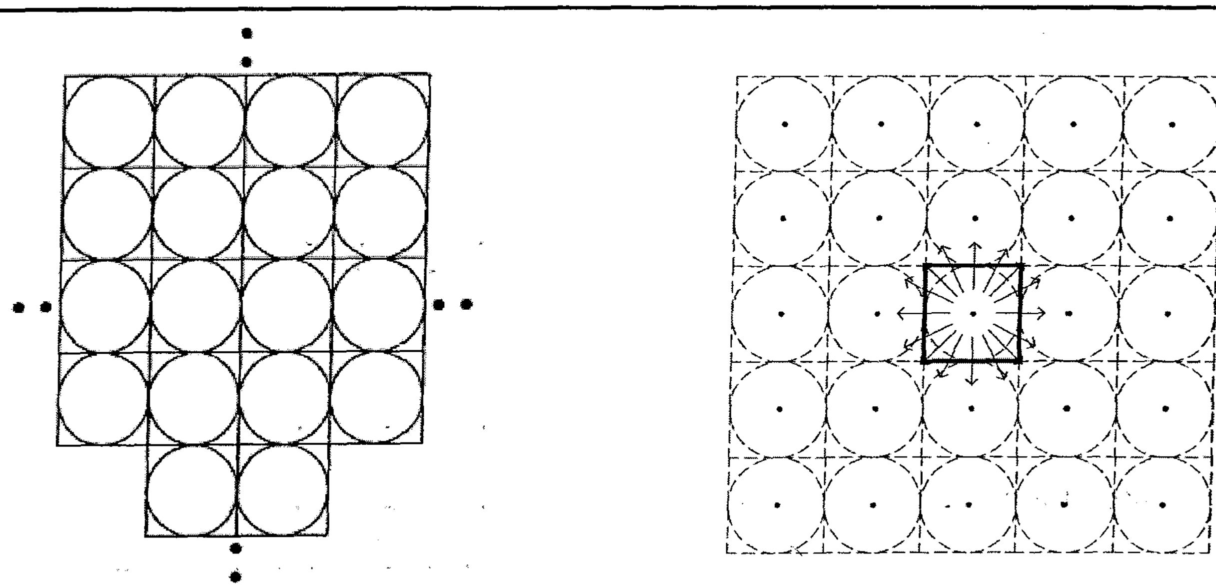

Tiling Pattern Using 2^M – Sided Regular Cell Fitted Within Square Tiles. Paired Dots Indicate Tiling Extending Beyond Illustration. Circles symbolize 2^M – Sided Polygons where m is very large, creating limiting Circle Cell.

Figure 5. Finite Difference Cell Flow Analog and Flow Directions for 2^M – Sided Regular Cell for Limiting Circle Cell Fitted within Square Tiles (note connection in any direction to closest element).

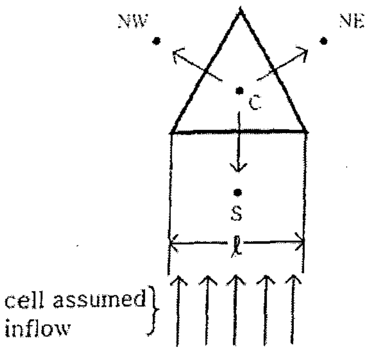

6a. Regular Square Cell

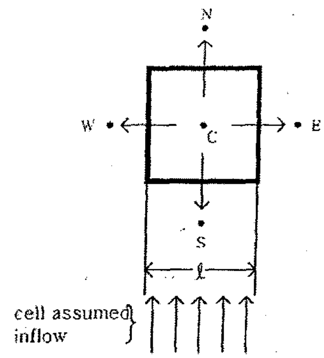

6b. Regular Triangle Cell

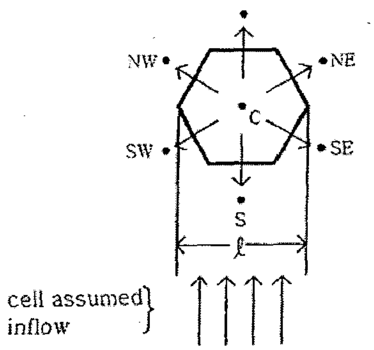

6c. Regular Hexagon Cell

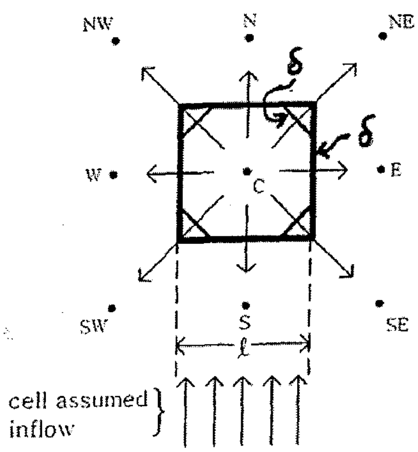

6d. Regular Octagon Cell Fitted in Grid Tile

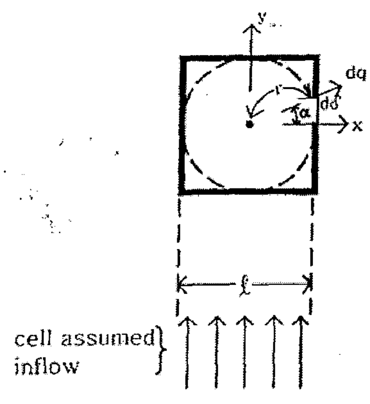

6e. Regular 2^M – Sided Cell (or Circle Cell) Fitted in Grid Tile

Figure 6. Cell Assumed Inflow and Outflow Directions.

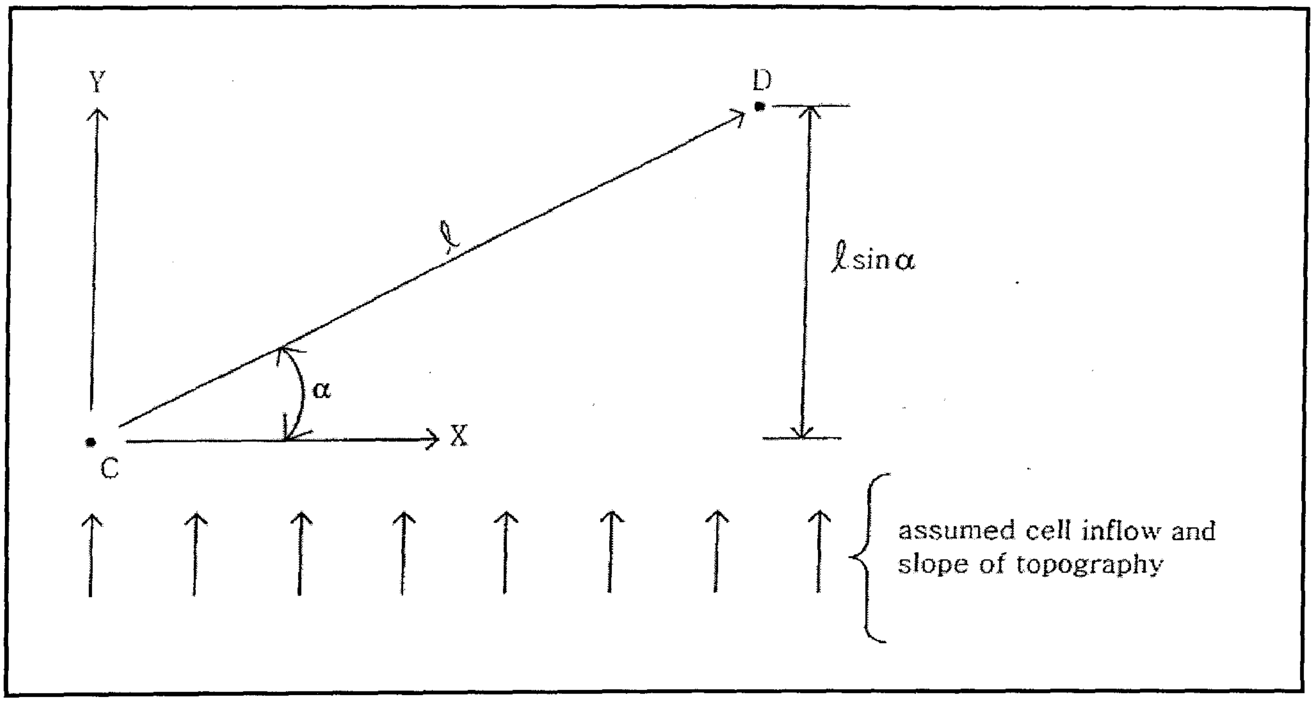

Figure 7. Calculations of Topographic Slope Along Flow Vector Between Nodes C and D.